# SPECTRAL VARIABILITY OF CYGNUS X-1 DURING AN INTERMEDIATE STATE

**J. Malzac[1], P.O. Petrucci[2], E. Jourdain[1], P. Sizun[3], M. Cadolle[3,4], G. Pooley[5], C. Cabanac[2], S. Chaty[3,6], T. Belloni[7], J. Rodriguez[3,6,8], J.P. Roques[1], P. Durouchoux[3], A. Goldwurm[3,4], and P. Laurent[3,4]**

[1]Centre d'Etude Spatiale des Rayonnements, (CNRS/OMP/UPS), 31028 Toulouse, France
[2]Laboratoire d'Astrophysique Observatoire de Grenoble, BP 53 F-38041 GRENOBLE Cédex 9, France
[3]Service d'Astrophysique, DSM/DAPNIA/SAp, CEA-Saclay, Bat. 709, L'Orme des Merisiers, F-91 191 Gif-sur-Yvette, Cedex, France
[4]APC-UMR 7164, 11 place M. Berthelot, 75231 Paris, France
[5]Cavendish Laboratory, University of Cambridge, Madingley Road, Cambridge CB3 0HE, UK
[6]AIM - Astrophysique Interactions Multi-échelles (Unité Mixte de Recherche 7158 CEA/CNRS/Université Paris 7 Denis Diderot), CEA-Saclay, Bât. 709, L'Orme des Merisiers, F-91 191 Gif-sur-Yvette Cedex, France
[7]INAF - Osservatorio Astronomico di Brera, via E. Bianchi 46, 23807 Merate, Italy
[8]INTEGRAL Science Data Center, Chemin d'Écogia 16, 1290 Versoix, Switzerland

## ABSTRACT

We report the results of a simultaneous radio (Ryle telescope) and hard X-ray *INTEGRAL* observation of Cygnus X-1 during an intermediate state. During the 4 day long observation the broad band (3–200 keV) luminosity varied by up to a factor of 2.6 and the source showed an important spectral variability. A principal component analysis demonstrates that most of this variability occurs through 2 independent modes. The first mode consists in changes in the overall luminosity on time scale of hours with almost constant spectra (responsible for 68 % of the variance) We interpret this variability mode as variations of the dissipation rate in the corona, possibly associated with magnetic flares. The second variability mode consists in a pivoting of the spectrum around $\sim$10 keV (27 % of the variance). It acts on a longer time-scale: initially soft, the spectrum hardens in the first part of the observation and then softens again. This pivoting pattern is strongly correlated with the radio (15 GHz) emission: radio fluxes are stronger when the *INTEGRAL* spectrum is harder We propose that the pivoting mode represents a 'mini' state transition from a nearly High Soft State to a nearly Low Hard State, and back. This mini-transition would be caused by changes in the soft cooling photons flux in the hot Comptonising plasma associated with an increase of the temperature of the accretion disc. The jet power then appears to be anti-correlated with the disc luminosity and unrelated to the coronal power.

Key words: Gamma-rays: observations –Black hole physics – Radiation mechanisms: non-thermal –X-rays: binaries; radio continuum: stars – X-rays: individual: Cygnus X-1 .

## 1. INTRODUCTION

Cygnus X-1 is the prototype of black hole candidates. Since its discovery in 1964 (Bowyer et al. 1965), it has been intensively observed by all the high-energy instruments, from soft X-rays to $\gamma$-rays. It is a persistent source most often observed in the so-called Low Hard State (hereafter LHS), characterised by a relatively low flux in the soft X-rays ($\sim$ 1 keV) and a high flux in the hard X-rays ($\sim$ 100 keV). In the LHS, the high-energy spectrum can be roughly described by a power-law with spectral index $\Gamma$ varying in the range 1.4-2.2, and a nearly exponential cut-off at a characteristic energy $E_{\rm c}$ of a few hundred keV (see e.g. Gierlinski et al. 1997). Occasionally, the source switches to the High Soft State (HSS). The high-energy power-law is then much softer ($\Gamma > 2.4$) and the bolometric luminosity is dominated by a thermal component peaking at a few keV. Finally, there are also Intermediate States (hereafter IMS) in which the source exhibits a relatively soft hard X-ray spectrum ($\Gamma \sim 2.1-2.3$) and a moderately strong soft thermal component (Belloni et al. 1996; Mendez & van der Klis 1997). The IMS often, but not always, appears when the source is about to switch from one state to the other. When it is not associated with a state transition, it is interpreted as a 'failed state transition'. (see Zdziarski et al. 2002, Pottschmidt et al. 2003, Gleissner et al. 2004).

Simultaneous radio/X-ray and high-energy observations of Cygnus X-1 and other sources have shown that the X-ray LHS is correlated with a strong radio emission which is consistent with arising from a jet (Fender 2001). In contrast, during HSS episodes the source appears to be radio weak (Brocksopp et al. 1999). The presence of a compact jet in the LHS was confirmed by Stirling et

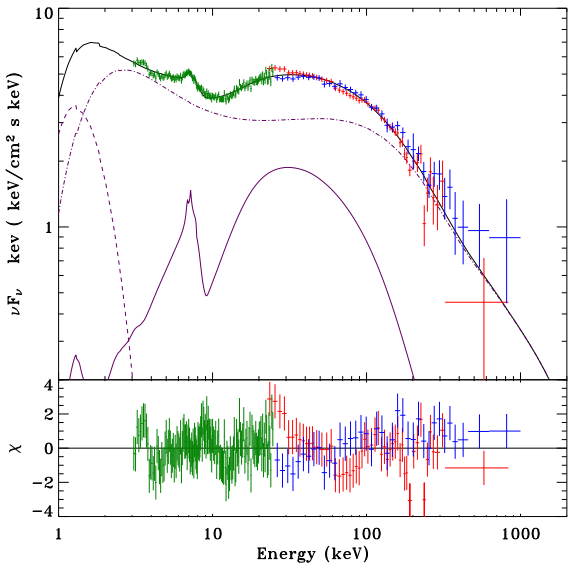


*Figure 1. Joint JEM-X/SPI/ISGRI spectrum of Cygnus X-1 averaged over revolutions 79 and 80. The data are fitted with the thermal/non-thermal hybrid Comptonisation model* EQPAIR *with* mono-energetic *injection of relativistic electrons with Lorentz factor. The lighter curves show the reflection component (solid), the disc thermal emission (dashed) and the Comptonised emission (dot-dash). The green, red and blue crosses show the JEM-X, IBIS/ISGRI and SPI data respectively The temperature of the inner disk (*DISKPN*) was fixed to $kT_{\rm max}$=0.3 keV in all fits. The soft photon compactness is fixed at $l_{\rm s} = 10$. The absorbing column density is $N_{\rm h} = 5 \times 10^{21}$ and the inclination angle 45 degrees. The resulting best fit parameters (see G99) are the folowing : hard to soft compactness ratio $l_{\rm h}/l_{\rm s}$=$0.85^{+0.02}_{-0.03}$, non-thermal to hard compactness ratio $l_{\rm nth}/l_h$=$0.51^{+0.04}_{-0.04}$, electron optical depth $\tau_{\rm p}$=$0.55^{+0.01}_{-0.06}$, injection Lorentz factor $\gamma_{\rm inj}$=$8.41^{+0.62}_{-0.92}$, reflection amplitude $\Omega/2\pi$ = $0.71^{+0.09}_{-0.03}$, reflection ionization parameter $\xi$=$525^{+143}_{-84}$ (erg cm $s^{-1}$), iron line energy and equivalent width $E_{\rm line}$=$7.02^{+0.32}_{-0.23}$ keV, EW= $90^{+38}_{-24}$ eV.*

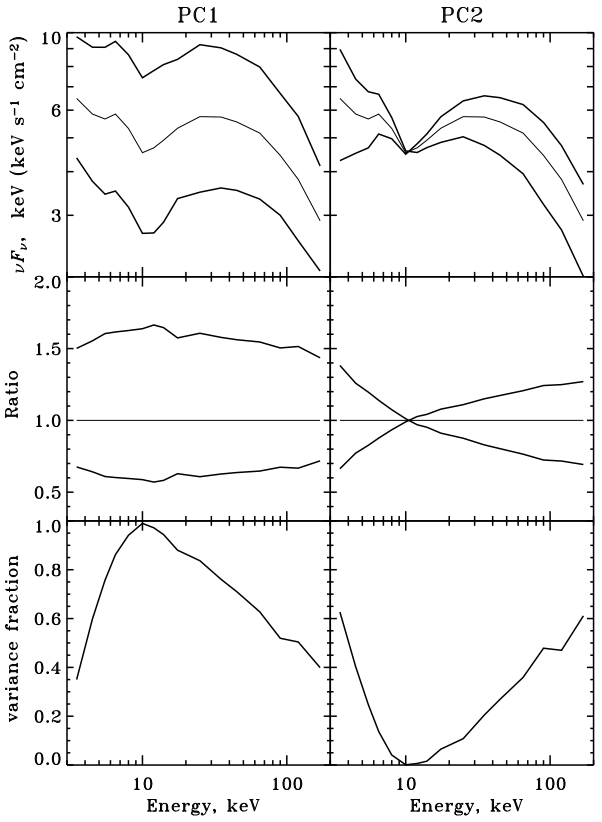


*Figure 2. The 2 principal components of variability. The upper panels illustrate the effects of the each component on the shape and normalisation of the spectrum: time average spectrum (light line) and spectra obtained for the maximum and minimum observed values of the normalisation parameter. The middle panels show the ratio of spectra obtained for the maximum and minimum normalisation to the average one. The bottom panels show the contribution of each component to the total variance as a function of energy.*

al. (2001) who presented evidence for an extended and collimated radio structure on milliarcsecond scales.

State transitions are generally interpreted as being associated with changes in the geometry of the accretion flow. In the HSS the geometrically thin optically thick disk (Shakura & Sunyaev 1973) extends down to the last stable orbit. The spectrum is dominated by the thermal disc component and peaks at a few keV. The hard X-ray emission is then believed to be produced in a non-thermal corona above and below the disc (Gierliński et al. 1999, hereafter G99). In the LHS the geometrically thin disc is truncated at a few hundred Schwarschild radii, the innermost part of the accretion flow forms a geometrically thick optically thin and hot disc (Shapiro et al. 1976; Narayan & Yi 1994) where high-energy radiation is produced trough thermal Comptonisation. During spectral transitions to the HSS the inner radius of the cold accretion disk decreases. This reduction of the inner disc radius is associated with either the cold disk penetrating inside the hot inner flow, or the later collapsing into an optically thick accretion disk with small active regions of hot plasma on top of it (Zdziarski et al. 2002). In both cases the enhanced soft photon flux from the disk tends to cool down the hot phase, leading to softer spectra.

Cygnus X-1 represents a prime target for the *INTEGRAL* mission and was extensively observed (Bouchet et al. 2003, Pottschmidt et al. 2003, Bazzano et al. 2003, Cadolle Bel et al., 2005). In this paper we focus on the results of the first observation of Cygnus X-1 in the open time programme. This 300 ks observation was performed on 2003 June 7-11 (rev 79/80) with a 5 × 5 dithering pattern[1] At this epoch, the *RXTE* All Sky Monitor count rate

[1] *INTEGRAL* observations are made of a succession of exposures of about 30 minute duration with varied pointed directions to enable *SPI*

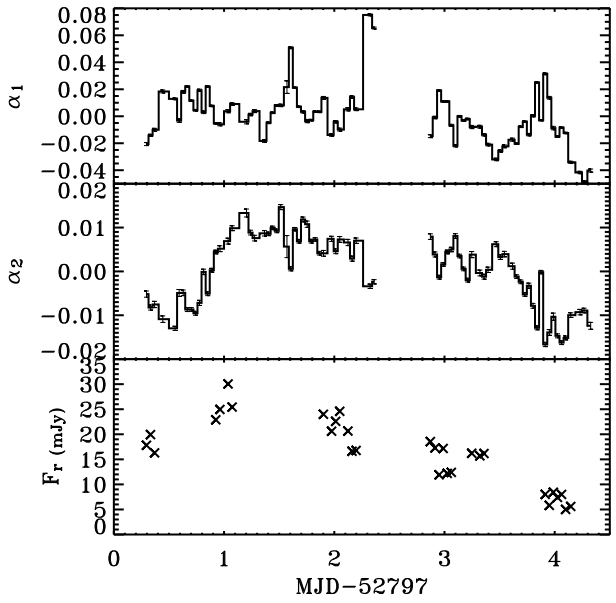


*Figure 3. Evolution of the parameters associated to PC 1 (top), PC 2 (middle) and radio light curve (bottom) during the observation*

of Cyg X-1 was higher than in typical LHS by up to a factor of 4, and the light curve showed strong X-ray activity characteristic of state (or failed state) transitions. We also combine the *INTEGRAL* data with the results of coordinated radio observations (15 GHz) performed with the Ryle telescope.

## 2. RESULTS

Fig. 1 shows the the joint *JEM-X*/*ISGRI*/*SPI* spectrum fitted with a thermal/non-thermal hybrid Comptonisation model (EQPAIR model (Coppi 1999; G99; Zdziarski et al. 2002, 2004) with mono energetic injection of non-thermal electrons. The unabsorbed best fit model spectrum is shown on Fig. 5. The apearence of the spectrum confirm that the source was in an IMS. Moreover, the resulting best fit parameters are intermediate between what is found in the LHS and HSS.

In order to study the spectral variability of the source during the observation, we produced light curves in 16 energy bands ranging from 3 to 200 keV with a time resolution of the duration of a science window (i.e. $\sim$ 30 min). The count rate in each band was then renormalised so that its time average matches the energy flux calculated from the best-fit model of the joint average *JEM-X*/*ISGRI*/*SPI* spectrum. Namely, for each energy band we compute the quantity $F(t) = \frac{\mathcal{C}(t)}{\bar{\mathcal{C}}}\bar{F}$, where $\mathcal{C}(t)$ is the mean count rate during pointing $t$, $\bar{\mathcal{C}}$ is the count rate averaged over the whole observation, $\bar{F}$ is the observation average energy flux in this band given by the best fit model. We use $F(t)$ as a proxy for the instantaneous energy flux, therefore neglecting the effects of the spectral variations on the instrumental response. The time averaged 3–200 keV model flux is $\bar{F}_{3-200} = 2.87 \times 10^{-8}$ ergs cm$^{-2}$ s$^{-1}$. The energy flux has a rms amplitude of 16 %, and the ratio of the maximum to the minimum luminosity is 2.6.

The light curves exhibit a complex and strong broad band variability of the spectra as well as the overall flux. We use a principal component analysis (PCA see e.g. Kendall, 1980) to seek for variability patterns in our sample. PCA finds $n$ independent components of the variability $C_1$ , $C_2$,...,$C_n$, so that the flux at energy $E_i$ and time $t_j$ can be written as follow:

$$F(E_i, t_j)) = \bar{F}(E_i) + \sum_{k=1}^{n} \alpha_k(t_j) C_k(E_i), \qquad (1)$$

where $\bar{F}(E_i)$ is the time averaged flux at energy $E_i$. The normalisation coefficients of each PCA component (respectively $\alpha_1$, $\alpha_1$,..., $\alpha_n$) vary in time. Their fluctuations (including negative values) account for the sample variance. On the other hand the $C_k$ coefficients are constant, they define the variability mode of each PCA component. The PCA components are ordered according to the amount of sample variance they account for (i.e. the observed fluctuations of $\alpha_1$ cause more variance than those of $\alpha_2$ which produce more variance than $\alpha_3$ etc...). The first few Principal Components (those representing most of the variance in the data) should reveal the shape of the relevant spectral components or variability modes. The higher order Principal Components might be expected to be dominated by the statistical and systematic noise in the spectra. To summarise, PCA finds the decomposition that maximises the variability due to lower order components, so that most of the variability can be described using a small number of components.

The results of our PCA analysis of the spectral variability of Cygnus X-1 are illustrated in Fig. 2, which shows how the 2 first principal components affect the flux and spectrum and their respective contribution to the total observed variance as a function of energy. As can be seen on this figure, the first principal component (PC 1) consists in a variability mode dominated by variations in the luminosity (normalisation) with little change in the spectral shape. For this reason, in the following, we will refer to PC 1 as the 'flaring mode'. This component accounts for 68 % of the sample variance. PC1 correlates very well with the high-energy flux. A least square fit shows that the 3-200 keV flux relates to $\alpha_1$ through:

$$F_{3-200} = \bar{F}_{3-200}(1 + 7.64\alpha_1), \qquad (2)$$

with a linear correlation coefficient of 0.98. So that $\alpha_1$ can be viewed as a tracer of the hard X-ray luminosity of the source.

As shown in Fig 2, the second PCA component (PC 2) can be described roughly as a pivoting of the spectrum

image deconvolution. Such a 30 minute pointing is called a science window

around 10 keV. The two spectra obtained for the minimum and maximum values of the $\alpha_2$ parameter controlling the strength of PC 2 are reminiscent of the canonical LHS and HSS spectra. This component is responsible for 27 % of the sample variance, and will be referred as the 'pivoting mode'. $\alpha_2$ can thus be seen as a tracer of the hardness of the high-energy spectrum.

Considered together the 2 first PCA components account for 95 percent of the observed variance. The remaining residual variability is entirely attributable to both statistical noise and instrumental effects. The intrinsic source variability is largely dominated by PC 1 (flaring mode) and PC 2 (pivoting mode). Fig. 3 shows the time evolution of the PCA parameters $\alpha_1$ and $\alpha_2$. $\alpha_1$, which traces the changes in bolometric luminosity at nearly constant spectra shows important variability on time scales of order of a few hours or less, but no clear systematic trend during the 4 days of observation. In contrast, $\alpha_2$, which roughly traces the hardness of the spectrum, seems to vary on longer time scales: it jumps during the first 2 days then decreases in the second part of the observation. This suggests that the physical mechanisms responsible for PC 1 and PC 2 are distinct (which is also expected from the fact that, by construction, PC 1 and PC 2 are linearly independent) and apparently acting on different time scales.

In order to study the possible correlations between the radio and hard X-ray emission, we selected the science windows for which we had simultaneous radio pointings. The resulting light curve is shown on the bottom panel of Fig. 3. Fig. 4 shows that the radio emission is strongly correlated to $\alpha_2$. The correlation is highly significant. The Spearman rank test correlation coefficient is 0.78 corresponding to a probability that the correlation is by chance of $2 \times 10^{-7}$. On the other hand, there is no hint of a correlation with the flaring mode as can be seen in the left panel of Fig. 4. In other terms, the radio emission is strongly correlated with the hardness and apparently unrelated to 2 to 200 keV luminosity.

## 3. DISCUSSION

We have shown that, during our IMS observation, the variability of Cygnus X-1 can be described by two independent variability modes:

On time-scales of a few hours or less there are important changes in luminosity with little spectral variations (flaring mode). On longer time scales there is a spectral evolution with the the spectrum pivoting around 10 keV.

We further showed that while there is no hint for a correlation between the radio flux and the flaring mode, the radio is strongly correlated with the pivoting of the spectrum, in the sense that the radio flux is stronger when the hard X-ray spectrum is harder.

Actually, the transition from LHS to HSS is known to be associated with a quenching of the radio emission (Corbel et al. 2000; Gallo, Fender & Pooley 2003). As the transition to the HSS also corresponds to a strong softening of the spectrum, this is consistent with the correlation between hardness and radio flux: when, during the observation, the source gets closer to the HSS the spectrum softens and simultaneously the radio flux decreases. Moreover, compilations of LHS and HSS spectra suggest that the spectral transition between LHS and HSS occurs through a pivoting around 10 keV (see e.g. Fig. 9 of McConnell et al 2002). The evolution of the $\alpha_2$ parameter shown in Fig. 3 indicates that the source, initially in a 'soft' IMS, switched to a harder state during the first 2 days of observation and then transited back toward a 'soft' state.

It is interesting to speculate on the cause of the two variability modes. We tried to reproduce such variability modes by varying the parameters of the hybrid thermal/non-thermal Comptonisation models shown in Fig. 1. As shown in the left panel of Fig. 5 it is possible to produce variations in luminosity by a factor comparable to what is observed and little spectral changes in the *INTEGRAL* band by varying the coronal compactness $l_{\rm h}$ by a factor of 2. In this context the flaring mode would correspond to variations of the dissipation rate in the corona possibly due to magnetic reconnection. This variability mode seems to be a characteristic of the HSS (Zdziarski et al. 2002). As we show here, it also provides a major contribution to the variability of the IMS.

Regarding the pivoting mode, it can be produced by changes in the flux of soft cooling photons at constant dissipation in the hot phase. We performed simulations assuming that the accretion disc radiates like a blackbody i.e. its flux $F_{disc} \propto l_{\rm s} \propto T_{\rm max}^4$ and constant $l_h$. For an increase of the disc temperature by a factor of 1.7, the disc luminosity grows by a factor of 8. As in this model, the disc flux also corresponds to the soft cooling photon input in the corona and the heating ($\propto l_{\rm h}$) is kept constant, this leads to a steepening of the spectrum with a pivot around 10 keV of similar amplitude as in PC 2 (see Fig. 5). For the 1996 HSS, G99 found a ratio $l_h/l_s \sim 0.3$ while in the LHS $l_h/l_s$ ranges between 3.5 to 15 (Ibragimov et al. 2005). The range of $l_h/l_s$ (0.4–3.4) required to reproduce the observed amplitude of the pivoting mode matches almost exactly the intermediate range between the HSS and the lower limit of the LHS. The source initially in a (quasi) HSS evolved toward the LHS but as soon as it was reached, it went back toward the HSS.

Since, in the *INTEGRAL* band, the constraints on disc thermal emission are loose we did not attempt to model the data with a varying inner disc radius which is, moreover, difficult to disentangle from fluctuations of the disc temperature. In the fitted models as well as the models shown in Fig. 5, the inner disc radius is fixed at 6 $R_g$. Nonetheless our result would also be consistent with the disc moving inward and outward of the hot phase during the state transitions. Indeed, when the inner disc radius is approaching the black hole, its maximum temper-

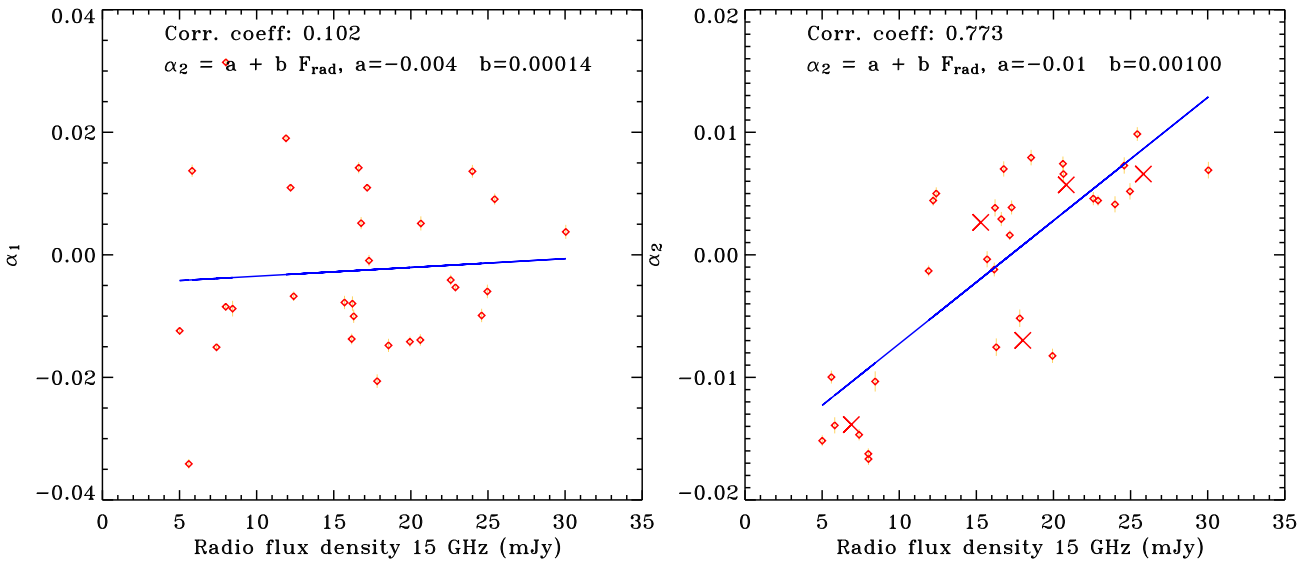


*Figure 4. PCA parameters $\alpha_1$ (left panel) and $\alpha_2$ (right panel) as a function of the radio flux (diamonds). In both panels, the best linear fits are shown by the solid lines. The crosses indicate the time average over each of the five periods of nearly continuous radio coverage (see Fig 3). While there is no convincing correlation between the radio flux and $\alpha_1$, the radio flux is correlated to $\alpha_2$ at highly significant level.*

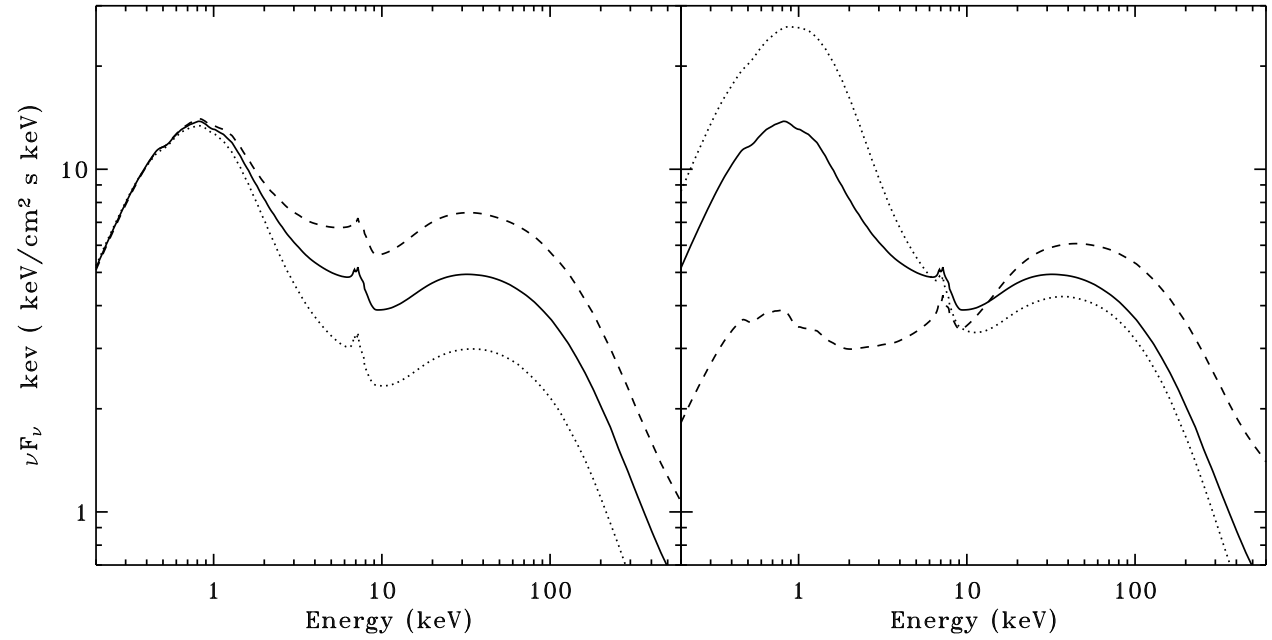


*Figure 5. Left panel: effect of varying $l_h$ by a factor of 2 on the* EQPAIR *model with monoenergetic injection (see Sect. 2). Solid curve: unabsorbed best-fit model ($l_h = 8.5$); Dotted curve $l_h = 5.7$; Dashed curve: $l_h = 11.9$. Right panel: effect of varying the soft photons flux by a factor of 8. Solid curve: unabsorbed best-fit model ($T_{\rm disc} = 0.3$ keV; $l_{\rm h}/l_{\rm s} = 0.85$). Dotted curve: $T_{\rm disc} = 0.357$ keV and $l_{\rm h}/l_{\rm s} = 0.42$. Dashed curve: $T_{\rm disc} = 0.212$ keV and $l_{\rm h}/l_{\rm s} = 3.4$.*

ature and luminosity increases[2] leading to a more efficient cooling of the hot flow/corona. The anti-correlation between radio flux and disc luminosity would be due to the jet expanding when the cold accretion disc recedes and then shrinking in the second phase of the observation when the disc moves back inward. It is interesting to note that the change in disc flux required (a factor of $\sim 8$) to explain the spectral evolution is comparable to the amplitude of the variations of the radio flux (a factor of $\sim 6$). This suggests a direct relation between the disc flux and jet power. The overall change in bolometric

[2]Unless the mass accretion rate is reduced by a larger amount, which seems very unlikely, the evidence being rather that the accretion rate is often (but not always) larger in the soft than in the LHS.

luminosity occuring during the PC2 transition estimated from the fiducial 'hard' and 'soft' state models shown on the left panel of Fig. 5, is about a factor of 2. Because of the relatively short time scale ($\sim$ a day) on which the variation in luminosity occurs, it is unlikely to be driven by changes in the mass accretion rate. Most probably, it is due to a change in the radiative efficiency of the flow. The accretion flow could be less efficient in the LHS, because about half of the accretion power is either swallowed by the black hole or pumped into the jet, while, in the HSS, the cold disc is expected to be radiatively efficient.

The evolution of the hard X-ray corona luminosity during our IMS observation is very puzzling. Indeed, if, as commonly believed for the LHS, the corona constitutes the base of the jet, it is difficult to conceive that changes in the jet power and/or extension is not associated to changes in the energetics of the corona. Similarly, one would expect the corona/hot accretion flow to respond to changes in the disc power and/or distance of the truncation radius. Instead, we infer dramatic changes in the jet and disc power that are anti-correlated with each other, but *completely unrelated* to the fluctuations of the coronal power.

## 4. CONCLUSION

During our observation, the source presented a strong flux spectral variability occurring through 2 independent variability modes: First, there are changes in the dissipation rate in the corona, due to local instabilities or flares, producing a variability of the hard X-ray luminosity on timescales of hours and no strong spectral alterations. Strikingly, this coronal activity seems to be unrelated to the evolution of the jet and cold disc luminosity. Second, we observe a slower 4-day evolution starting from a spectrum close to the canonical HSS toward an almost LHS and back. This spectral evolution was characterized by a pivoting of the spectrum around 10 keV. It was correlated with the radio emission which was stronger when the hard X-ray spectrum was harder. It is interpreted in terms of a variable soft cooling photon flux in the corona associated with changes in the thermal disc luminosity and radio-jet power. This interpretation suggests a jump in bolometric luminosity of about a factor of 2 during the transition from LHS to HSS, which might indicates that the LHS accretion flow is radiatively inefficient, half of the accretion power being possibly advected into the black hole and/or the radio jet.

## ACKNOWLEDGMENTS

This paper is based on observations with *INTEGRAL*, an ESA project with instruments and science data centre funded by ESA member states (especially the PI countries: Denmark, France, Germany, Italy, Switzerland, Spain), Czech Republic and Poland, and with the participation of Russia and the USA. The Ryle Telescope is supported by PPARC.

## REFERENCES

[1] Bazzano, A., et al. 2003, A&A, 411, L389

[2] Belloni, T., Mendez, M., van der Klis, M., et al., 1996, ApJ, 472, L107

[3] Bouchet L., et al. 2003, A&A, 411, L377

[4] Bowyer, S., Byram, E.T., Chubb, T.A., Friedman, M., 1965, Sci, 147, 394

[5] Brocksopp, C., Fender, R. P., Larionov, V., Lyuty, V. M., Tarasov, A. E., Pooley, G. G., Paciesas, W. S., & Roche, P. 1999, MNRAS, 309, 1063

[6] Cadolle Bel, M., Sizun, P., Goldwurm, A., Rodriguez, J., Laurent, P., Zdziarski, A. A., Foschini, L., Goldoni, P., Gouiffes, C., Malzac, J., Roques, J.P.R., 2005, A&A submitted (CB05)

[7] Corbel, S., et al., 2000, A&A, 359, 251

[8] Coppi, P. S. 1999, ASP Conf. Ser. 161: High Energy Processes in Accreting Black Holes, 161, 375

[9] Fender, R. P. 2001, MNRAS, 322, 31

[10] Gallo, E., Fender, R. P., & Pooley, G. G. 2003, MNRAS, 344, 60

[11] Gierliński, M., et al., 1997, MNRAS, 288, 958

[12] Gierliński, M., Zdziarski, A. A., Poutanen, J., Coppi, P. S., Ebisawa, K., & Johnson, W. N. 1999, MNRAS, 309, 496 (G99)

[Kendall 1980] Kendall, M. G., 1980, "Multivariate Analysis", Second Edition, Charles Griffin and Co. London.

[13] McConnell, M. L., et al. 2002, ApJ, 572, 984

[14] Mendez, M. & van der Klis, M. 1997, ApJ, 479, 926

[15] Narayan, R., & Yi, I. 1994, ApJ, 428, L13

[16] Pottschmidt, K., et al. 2003, A&A, 411, L383

[17] Shakura, N. I. , & Sunyaev, R. A., 1973, A&A, 24, 337

[18] Shapiro, S. L., Lightman, A. P., & Eardley, D. M., 1976, ApJ, 204, 187

[19] Stirling, A. M., Spencer, R. E., de la Force, C. J., Garrett, M. A., Fender, R. P., & Ogley, R. N. 2001, MNRAS, 327, 1273

[20] Zdziarski, A. A., Poutanen, J., Paciesas, W. S., & Wen, L. 2002, ApJ, 578, 357

[21] Zdziarski, A. A., Gierliński, M., Mikołajewska, J., Wardziński, G., Smith, D. M., Alan Harmon, B., & Kitamoto, S. 2004, MNRAS, 351, 791